ORIGINAL ARTICLE

Integrative "Omic" Analysis of Experimental Bacteremia Identifies a Metabolic Signature That Distinguishes Human Sepsis from Systemic Inflammatory Response Syndromes

Raymond J. Langley[1]*, Jennifer L. Tipper[2]*, Shannon Bruse[3], Rebecca M. Baron[4], Ephraim L. Tsalik[5,6,7], James Huntley[8], Angela J. Rogers[4,9], Richard J. Jaramillo[2], Denise O'Donnell[2], William M. Mega[10], Mignon Keaton[11], Elizabeth Kensicki[11], Lee Gazourian[4], Laura E. Fredenburgh[4], Anthony F. Massaro[4], Ronny M. Otero[12], Vance G. Fowler, Jr.[6,7], Emanuel P. Rivers[12], Chris W. Woods[6,7,13], Stephen F. Kingsmore[14,15], Mohan L. Sopori[1], Mark A. Perrella[4], Augustine M. K. Choi[4], and Kevin S. Harrod[2]

[1]Respiratory Immunology Program, [2]Infectious Diseases Program, [3]COPD Program, and [10]Applied Life Sciences and Toxicology, Lovelace Respiratory Research Institute, Albuquerque, New Mexico; [4]Pulmonary Division, Brigham and Women's Hospital, Boston, Massachusetts; [5]Emergency Medicine and Research Services and [13]Medicine Service, Durham Veterans Affairs Medical Center, Durham, North Carolina; [6]Department of Medicine, Duke University School of Medicine, Durham, North Carolina; [7]Institute for Genome Sciences and Policy, Duke University, Durham, North Carolina; [8]Advanced Genomics Biofrontiers Institute, University of Colorado, Boulder, Colorado; [9]Channing Laboratory, Boston, Massachusetts; [11]Metabolon, Inc., Durham, North Carolina; [12]Department of Emergency Medicine, Henry Ford Health Systems, Detroit, Michigan; and [14]Center for Pediatric Genomic Medicine, Children's Mercy Hospitals and Clinics, and [15]Department of Pediatrics, University of Missouri-Kansas City School of Medicine, Kansas City, Missouri

Abstract

Rationale: Sepsis is a leading cause of morbidity and mortality. Currently, early diagnosis and the progression of the disease are difficult to make. The integration of metabolomic and transcriptomic data in a primate model of sepsis may provide a novel molecular signature of clinical sepsis.

Objectives: To develop a biomarker panel to characterize sepsis in primates and ascertain its relevance to early diagnosis and progression of human sepsis.

Methods: Intravenous inoculation of *Macaca fascicularis* with *Escherichia coli* produced mild to severe sepsis, lung injury, and death. Plasma samples were obtained before and after 1, 3, and 5 days of *E. coli* challenge and at the time of killing. At necropsy, blood, lung, kidney, and spleen samples were collected. An integrative analysis of the metabolomic and transcriptomic datasets was performed to identify a panel of sepsis biomarkers.

Measurements and Main Results: The extent of *E. coli* invasion, respiratory distress, lethargy, and mortality was dependent on the bacterial dose. Metabolomic and transcriptomic changes characterized severe infections and death, and indicated impaired mitochondrial, peroxisomal, and liver functions. Analysis of the pulmonary transcriptome and plasma metabolome suggested impaired fatty acid catabolism regulated by peroxisome-proliferator activated receptor signaling. A representative four-metabolite model effectively diagnosed sepsis in primates (area under the curve, 0.966) and in two human sepsis cohorts (area under the curve, 0.78 and 0.82).

Conclusions: A model of sepsis based on reciprocal metabolomic and transcriptomic data was developed in primates and validated in two human patient cohorts. It is anticipated that the identified parameters will facilitate early diagnosis and management of sepsis.

Keywords: metabolomics; transcriptomics; bacteremia; nonhuman primates; mitochondrial dysfunction

(Received in original form April 2, 2014; accepted in final form July 17, 2014)

*These authors contributed equally.

Supported by National Institutes of Health for CAPSOD (U01AI066569, P20RR016480, HHSN266200400064C) and RoCI (HL112747 and HL05530). E.L.T. was supported by Award #1IK2CX000530 from the Clinical Science Research and Development Service of the Veterans Health Administration Office of Research and Development.

Author Contributions: Funding, S.F.K., V.G.F., E.P.R., C.W.W., A.M.K.C., and E.L.T. Study design, J.L.T., R.J.L., R.M.B., M.A.P., A.M.K.C., and K.S.H. Experimental procedures, R.J.L., J.L.T., R.M.B., R.J.J., D.O., W.M.M., E.L.T., A.J.R., L.G., L.E.F., A.F.M., and S.F.K. Sequencing, J.H. Metabolomics, R.J.L., M.K., and E.K. Bioinformatics and statistical analysis, S.B. and R.J.L. CAPSOD clinical analysis and study design, R.J.L., E.L.T., R.M.O., V.G.F., E.P.R., C.W.W., and S.F.K. RoCI clinical analysis and study design, R.M.B., A.J.R., L.G., L.E.F., A.F.M., and A.M.K.C. Manuscript preparation, R.J.L., J.L.T., R.M.B., E.L.T., A.J.R., S.F.K., M.L.S., M.A.P., and K.S.H.

Correspondence and requests for reprints should be addressed to Kevin Harrod, Ph.D., 2425 Ridgecrest Drive SE, Albuquerque, NM 87108. E-mail: kharrod@lrri.org; effective October 15, 2014: Department of Anesthesiology, School of Medicine, University of Alabama at Birmingham, 619 19th Street S, Birmingham, AL 35249.

This article has an online supplement, which is accessible from this issue's table of contents at www.atsjournals.org

Am J Respir Crit Care Med Vol 190, Iss 4, pp 445–455, Aug 15, 2014

Originally Published in Press as DOI: 10.1164/rccm.201404-0624OC on July 23, 2014
Internet address: www.atsjournals.org

At a Glance Commentary

Scientific Knowledge on the Subject: Sepsis and septic shock represent leading contributors to mortality and morbidity in intensive care units. Multiorgan dysfunction and failure are central to sepsis, but the mechanism and biomarkers of sepsis severity are largely unknown. For proper patient management, intensivists and trauma physicians need diagnostic tests that can distinguish among a systemic inflammatory response syndrome, sepsis, and trauma.

What This Study Adds to the Field: Metabolomics, an emerging approach to survey the entire organismal system, was used to elucidate the molecular signatures in experimental sepsis. The markers identified from this analysis represented components of broader metabolomic changes and distinguished noninfected SIRS from sepsis with greater than 90% accuracy in two human patient cohorts.

Clinical sepsis is defined by the presence of two or more criteria of the systemic inflammatory response syndromes (SIRS) in a patient with an infection (1, 2). Clinical sepsis is a complex, heterogeneous disease with a high, but variable mortality that accounts for more than half of all in-hospital deaths (3). The disease is influenced by the site of infection, causative organism, acute organ dysfunction, and underlying comorbidities (1, 2). The variability of sepsis and lack of specific symptoms make it difficult for physicians to make an early diagnosis or estimate of prognosis, both of which are necessary for optimal treatment. Some patients have severe sepsis (sepsis complicated by organ dysfunction) when first seen by a physician and yet improve without intensive therapy, whereas others with mild symptoms may rapidly progress to septic shock (hypotension refractory to fluid resuscitation or hyperlactatemia) or death.

Early goal-directed therapy (EGDT) has improved sepsis outcomes through a management protocol designed to provide antibiotics and optimize cardiac function and oxygen delivery within the first 6 hours of developing hypotension or cryptic shock (4). Accurate diagnosis is critical because delayed therapy in patients that do not meet the criteria for the initiation of EGDT at presentation accounts for up to 56% of in-hospital sepsis deaths (3). Conversely, aggressive microbial therapy can also have negative side effects (5). Withholding antibiotic treatment in surgical intensive care unit (ICU)–acquired sepsis until confirmatory microbiologic data may improve mortality and reduce the risk of microbial resistance (6, 7). Better identification of patients that benefit from aggressive therapy versus those that would benefit from a more conservative approach will likely improve patient management and reduce the risk of antimicrobial resistance in hospital ICUs (2).

We have previously demonstrated that metabolomic markers implicate mitochondrial dysfunction and that a clinicometabolomic model of sepsis can more accurately predict outcomes than lactate, Sequential Organ Failure Assessment, or Acute Physiology and Chronic Health Evaluation II scores (8). However, the model lacked temporal dynamics to determine diagnosis and matched peripheral transcriptomics analysis to implicate host genomic responses as underlying mechanisms. With this in mind, we performed a holistic integrative analysis (9) of transcriptomic and metabolomic changes of infected nonhuman primates (NHP) to identify novel underlying pathophysiology and develop a metabolomic diagnostic panel that can better predict sepsis than current methods. Some of these results have been previously reported in the form of an abstract (10).

Methods

Detailed methods are contained in the online supplement.

Animals

The protocol and amendments established for this study were reviewed and approved by The Lovelace Respiratory Institute's Animal Care and Use Committee and adhered to guidelines established by the American Association for the Accreditation of Laboratory Animal Care.

Human Subjects

The Community-acquired Pneumonia and Sepsis Outcomes Diagnostic (CAPSOD) study was approved by the Institutional Review Boards of the National Center for Genome Resources, Duke University Medical Center, Durham Veterans Affairs Medical Center, and Henry Ford Health Systems and filed at ClinicalTrials.gov (NCT00258869) (8, 11–13). The Registry of Critical Illness (RoCI) is approved by the Partners Human Research Committee under IRB protocol 2008-P-000495 (14, 15).

Method Summary

Our model in cynomolgus macaques was a modification of that described by Welty-Wolfe and coworkers (16). Baseline plasma measurements from 26 animals served as a control. Twenty-four animals were then challenged with heat-killed *Escherichia coli* bacteria approximately 12 hours before an infusion of live *E. coli* (*see* Table E1 in the online supplement). We preferred the "two-hit" infection model over a single-infusion model because the hypotension observed with live *E. coli* challenge is attenuated by the prime, allowing more opportunity for acute lung injury resembling sepsis-induced acute respiratory distress syndrome (17, 18). The *E. coli* O1:K1:H7 strain (American Type Culture Collection) was chosen given its activity as an extraintestinal pathogen and uropathogen (19, 20) when administered intravenously, along with demonstrated survival and growth outside of an intestinal environment (21). Animals were observed post-challenge for the onset of clinical symptoms. Animals inoculated with *E. coli* that became moribund were killed. Samples obtained when animals were clinically ill because of sepsis were labeled as "infection," but if sampled during convalescence, then they were labeled as "noninfection." Histopathology, metabolomics, RNAseq expression experiments and analyses, statistical analysis, the Database for Annotation, Visualization and Integrated Discovery (DAVID) pathway analysis (22, 23), and global cross-correlation analysis are described in detail in the online supplement. Metabolomic studies were performed by Metabolon, Inc. (Durham, NC). RNAseq was performed on a HiSeq2000 at the BioFrontiers Institute (University of Colorado, Boulder, CO). Statistical analysis was performed using JMP Genomics 5.1 (SAS Institute Inc., Cary, NC).

Results

To understand the molecular signatures of sepsis in the plasma metabolome we performed an infection challenge in NHPs. Twenty-four cynomolgus macaques (*Macaca fasciculari*) were primed with a heat-killed inoculation of *E. coli* (10^5–10^9 CFU) in the blood followed 12 hours later by challenge with live enteropathogenic *E. coli* (10^5–10^{12}) (*see* Table E1) (16). A dose range was chosen to avoid infusion shock (21) and to promote a gradient of responses. However, four monkeys did succumb at the time of infusion. Although these may represent "infusion deaths," they were conservatively removed from further analysis other than baseline metabolomics. Two animals were used for baseline transcriptomic profiling. The remaining animals were monitored for up to 5 days post-challenge. Plasma was taken at baseline (7 d before challenge), and at 1, 3, and 5 days, or before euthanasia for moribund animals (*see* Table E1). Few clinical manifestations of illness were noted in low-dose challenges (prime, 1×10^5 to 1×10^8; live, 1×10^4 to 5×10^9). In contrast, high-dose challenges (prime, 1×10^9; live, 1×10^{10} to 5×10^{12}) led to respiratory distress, lethargy, and death (Figure 1A). Bacteria could be cultured from plasma, lungs, spleen, and kidney in some low-dose and all high-dose challenges (*see* Table E1; Figure 1). A dose–response effect was observed with mortality, increased lung weight, and histologic lung injury at higher bacterial titers (Figure 1). Lung histopathology revealed bacteria with a concomitant lung inflammation, septal wall thickening, and proteinaceous exudates consistent with pneumonia. Focal lung hemorrhage was noted in the two highest doses.

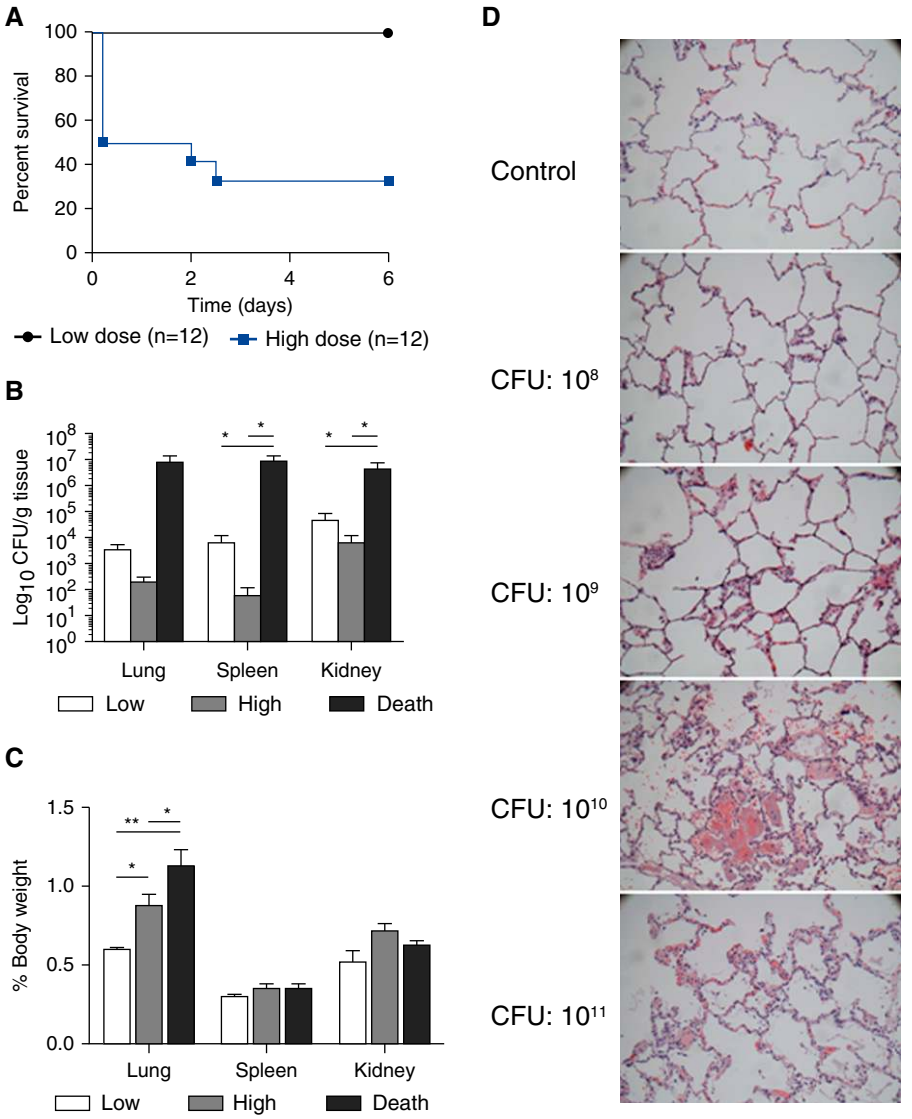

Figure 1. *Escherichia coli* challenge of cynomolgus macaques leads to increased mortality, tissue colonization, and inflammation in a dose-dependent manner. (*A*) Kaplan-Meier curve for live *E. coli* challenge. Low-dose challenge (prime, 1×10^5 to 1×10^8; live, 1×10^4 to 5×10^9); high-dose challenge (prime, 1×10^9; live, 1×10^{10} to 5×10^{12}). Four animals in the high-dose range died shortly after live infusion (1–2 h) and were not included in subsequent analyses other than for baseline metabolomics. (*B*) *E. coli* tissue colony-forming units from animals after killing in low-dose challenge (low), high-dose challenge (high) survivors, and death. $^*P < 0.05$. Necropsy of all animals was performed at 5 days post-challenge, except for the animals that were killed because of moribund state at 6–60 hours post-challenge. (*C*) Relative tissue mass after killing. $^*P < 0.05$; $^{**}P < 0.001$. (*D*) Lung sections (×200) were examined blindly for histologic evidence of lung injury. Control animals demonstrated normal lung architecture, animals in the low-dose challenge (CFU 10^8, CFU 10^9) groups exhibited mild inflammation and interstitial edema, and animals in the high-dose challenge (CFU 10^{10}, CFU 10^{11}) groups exhibited pronounced tissue injury with lung inflammation and edema.

Metabolomic Analysis in NHP Plasma

Global plasma metabolite analysis using semiquantitative mass spectrometry (8) was performed in preinfection (baseline) and postinfection (1, 3, and 5 d) plasma (Figure 2A). We used a multivariate technique known as unsupervised principal components analysis, using Pearson product-moment correlation coefficient, which allows us to examine relationships among many quantitative variables by three-dimensional clustering. The plasma metabolomic differences clustered in concordance with illness duration and severity (Figures 2B and 2C). Analysis of variance (all pairwise comparisons, 5% false discovery rate [FDR] [24, 25]) found that 127 of 349 (36.4%) metabolites were significantly different in the low-dose challenge, whereas 188 metabolites (53.9%) were significantly different in high-dose/fatal sepsis comparisons (*see* Table E2). Most metabolite concentrations returned close to baseline by 5 days in survivors (Figures 2D–2J).

To determine if the experimental model reflected changes found in human sepsis we first looked at lactate concentration, a clinical marker used for the initiation of EGDT (4, 26). Lactate was

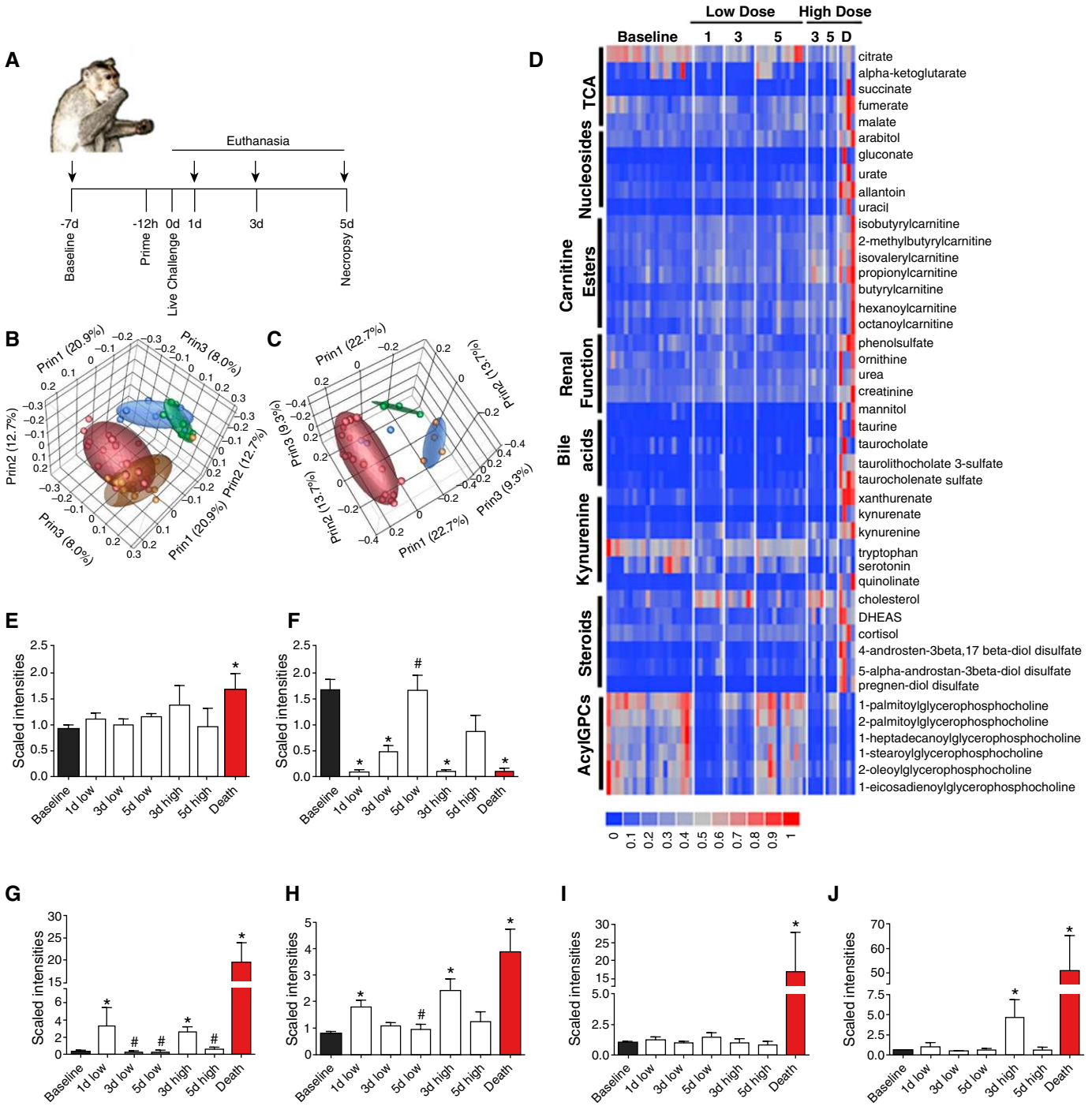

Figure 2. Metabolomic changes in nonhuman primates (NHP) two-hit sepsis model. (*A*) Experimental design. *Arrows* indicate the time blood was collected. Scaled metabolomic intensities were log2+1 transformed, and analysis of variance with 5% false discovery rate was performed against time course of low-dose challenge (baseline, n = 20; 1 d post-challenge, n = 7; 3 d post-challenge, n = 7; 5 d post-challenge, n = 12) or high-dose sepsis challenge (baseline, n = 20; 3 d post-challenge, n = 4; 5 d post-challenge, n = 3; and death, n = 4). Unsupervised principal components analysis using Pearson moment correlation for (*B*) infection low-dose comparison (baseline, *red*; 1 d post-challenge, *green*; 3 d post-challenge, *blue*; 5 d post-challenge, *gold*) and (*C*) infection high-dose comparison (baseline, *red*; 3 d post-challenge, *green*; 5 d post-challenge, *blue*; death, *gold*). (*D*) Cell plot of significant metabolomic changes affected by sepsis grouped by metabolic pathway. (*E*–*J*) Bar charts of representative metabolic pathways affected by sepsis challenge (*E*, lactate; *F*, 1-stearoyl-glycerophosphocholine; *G*, taurolithocholate-3-sulfate; *H*, isovalerylcarnitine; *I*, succinate; *J*, pregnen-diol disulfate). *Significantly different from control. #Significantly different comparison 1–5 d low-dose, or 3–5 d high-dose. Low-dose comparison (−log10 *P* value ⩾ 2.14) or high-dose comparison (−log10 *P* value ⩾ 2.00). TCA = tricarboxylic acid.

moderately increased in fatal cases but was insensitive to temporal changes despite bacteremia and histopathologic evidence of infection (Figures 2D and 2E; *see* Table E2). The lack of significant lactate changes in low- and high-dose survivors suggests the animals were able to maintain adequate organ perfusion despite the infection. We then took an unbiased approach to identify sepsis biomarkers by comparing the metabolomes at baseline with temporal changes in survivors and nonsurvivors.

We identified six distinct metabolic pathways with dynamic changes in regards to sepsis diagnosis and severity (e.g., death) and that are similar to clinical sepsis (8): (*1*) decreased acyl-glycerophosphocholines (acyl-GPCs); (*2*) increased kynurenine derivatives; (*3*) increased bile acids; (*4*) increased carnitine esters; (*5*) increased tricarboxylic acid (TCA) cycle intermediates; and (*6*) increased pregnen-sulfated and androgenic steroids (Figures 2 and 3; *see* Table E2). The metabolomic changes in five of these six pathways represented a graded response with the most dynamic changes noted in the samples taken from moribund animals. For moribund animals, the plasma concentrations of carnitine esters, conjugated bile acids, TCA intermediates, and kynurenine derivatives were significantly increased over the 3-day high-dose challenge samples (*see* Table E2). Acyl-GPCs, however, are similarly decreased at infection regardless of severity. Of these six pathways, four are already known to play a prominent role in sepsis. For example, acyl-GPCs have been suggested in sepsis diagnosis (27) and treatment (28); whereas kynurenine, a known immunosuppressive metabolite, is a biomarker for active tuberculosis infections (29). Increased conjugated bile acids (e.g., taurocholenate and taurolithocholate-3 sulfate) have been identified as sensitive indicators of sepsis-induced cholestasis and poor outcomes (30). We previously observed increases in small-chain, medium-chain, and branched-chain amino acid (BCAA) carnitine esters, consistent with the finding that dysregulated β-oxidation and BCAA degradation precedes sepsis-induced death

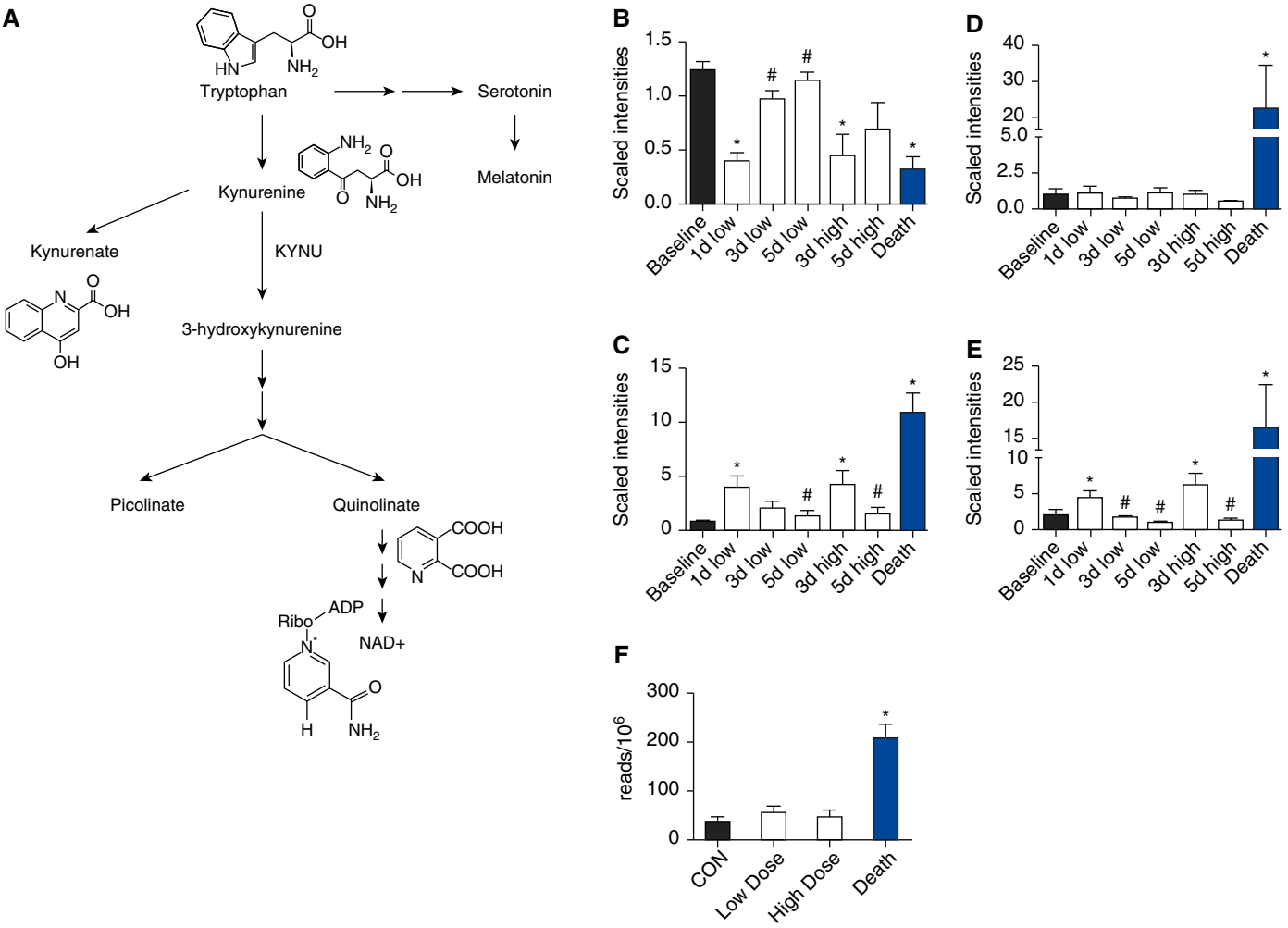

Figure 3. Kynurenine pathway modification. (*A*) Kynurenine metabolic pathway. (*B–E*) Bar charts of raw scaled metabolic data for tryptophan (*B*), kynurenine (*C*), kynurenate (*D*), and quinolinate (*E*). Analysis of variance (5% false discovery rate). *Significantly different from control, #Significantly different comparison 1–5 d low-dose or 3–5 d high-dose. Low-dose comparison (−log10 *P* value ⩾ 2.14) or high-dose comparison (−log10 *P* value ⩾ 2.00). (*F*) Bar chart for transcriptomic counts data for kynureninase (KYNU) in control (CON), low-dose challenge, high-dose challenge, and death. *−Log10 *P* value ⩾ 3.00.

(8). The results suggest that the primate model and human results share a similar metabolomic response in sepsis.

Lung Transcriptomic Response Caused by Severe *Escherichia coli* Infections

In light of the lung colonization and injury, lung transcriptomics were assessed across all infectious doses. RNAseq digital gene expression analysis was performed on RNA isolated from harvested lungs in uninfected control animals (n = 2), at necropsy (5-d low-dose, n = 8; 5-d high-dose, n = 4), or at killing for moribund state (n = 4; sepsis death) (Figure 4A; *see* Table E1). On average, $7.14 \times 10^6 \pm 0.41 \times 10^6$ total reads per sample aligned to the macaque transcriptome for a total of 17,476 expressed genes (*see* METHODS in the online supplement). A total of 1,544 genes were differentially expressed (all pairwise comparisons, analysis of variance, 3% FDR) (Figure 3C; *see* Table E3). Despite the fact that the baseline control animals were female (n = 2), whereas all low-dose challenge animals were male (n = 8), there were only six genes that were significantly different (*see* Table E2), which is consistent with human results (31). This suggested that the low-dose survivors had few sex-related differences and that the transcriptome had returned to near baseline in the low-dose survivors. The low-dose survivors provide a well-powered comparison between high-dose survivors and nonsurvivors while still in an early stage of convalescence. Significant differences were noted between the 5-day low-dose survivors and the 5-day high-dose survivors (n = 448), 5-day low-dose survivors and nonsurvivors (n = 754), and 5-day high-dose survivors and nonsurvivors (n = 662) (Figure 4B; *see* Table E3).

To understand the unbiased pathophysiologic changes caused by infection in both survivors and nonsurvivors we used a functional gene annotation tool known as DAVID to help define the biologic relevance of the 1,544 significantly different genes (22, 23). DAVID identified 109 pathways that were enriched because of the *E. coli* challenge in either high-dose survivors or nonsurvivors. Gene ontology of 15 pathways identified the mitochondria, peroxisome, fatty acid metabolism, BCAA-degradation, transcription factors, and inflammation as important pathways involved in sepsis survival and death (Figure 4D; *see* Table E4). The results suggest a genomic response that may

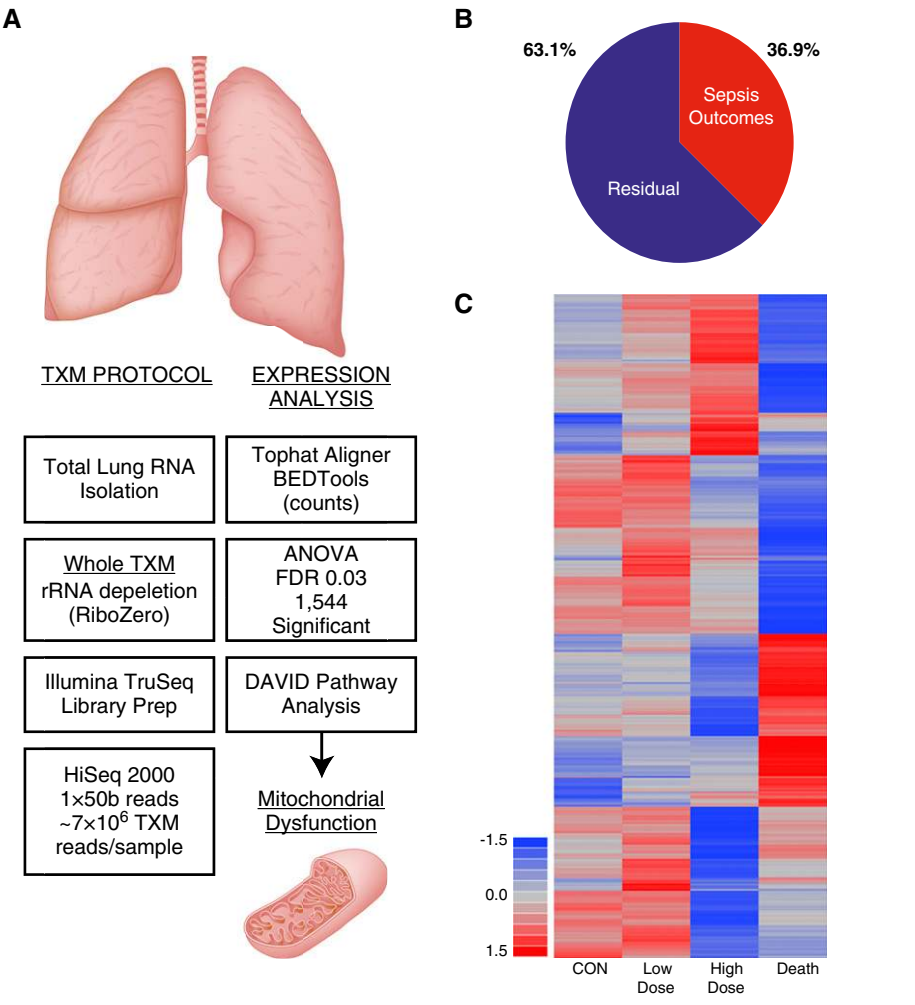

D

Category	Term	Count	PValue	Fold Enrichment	FDR
GOTERM_CC_FAT	Peroxisome	19	0.00002	3.199	0.030
GOTERM_CC_FAT	Mitochondrion	95	0.00003	1.516	0.050
GOTERM_MF_FAT	Cofactor binding	32	0.00011	2.112	0.176
GOTERM_BP_FAT	fatty acid metabolic process	27	0.00015	2.258	0.269
KEGG_PATHWAY	NOD-like receptor signaling pathway	13	0.00059	3.173	0.723
KEGG_PATHWAY	Propanoate metabolism	9	0.00085	4.256	1.035
GOTERM_BP_FAT	Programmed cell death	58	0.00065	1.572	1.172
GOTERM_BP_FAT	Cell death	65	0.00106	1.497	1.900
INTERPRO	Acyl-CoA oxidase/dehydrogenase type1/2 C-terminal	6	0.00127	6.793	2.094
KEGG_PATHWAY	Valine leucine and isoleucine degradation	10	0.00190	3.440	2.306
SP_PIR_KEYWORDS	Inflamation	7	0.00207	5.033	2.973
SP_PIR_KEYWORDS	Zinc-finger	123	0.00269	1.287	3.857
KEGG_PATHWAY	PPAR signaling pathway	12	0.00496	2.632	5.922
GOTERM_BP _FAT	Inflammatory response	33	0.00430	1.681	7.514
GOTERM_BP_FAT	Response to corticosteroid stimulus	13	0.00483	2.532	8.406

Figure 4. Transcriptomic analysis of whole-lung RNA. (*A*) Experimental design: total RNA was isolated from whole lungs, Truseq multiplex sequence libraries were built using rRNA depletion rather than poly-A selection. Samples were sequenced and aligned with Tophat and read counts were determined using BedTools. Analysis of variance (ANOVA) (false discovery rate = 0.03) was performed and significant gene lists were uploaded into the Database for Annotation, Visualization and Integrated Discovery (DAVID) with results suggesting mitochondrial dysfunction. (*B*) Venn diagram of significant differences in high-dose challenge versus low-dose challenge, low-dose

lead to metabolic and mitochondrial dysfunction in energy production in high-dose and lethal challenges and that the lung at least partially contributes to the systemic metabolic changes observed in the plasma. Several of the 94 enriched pathways (e.g., nucleotide-binding oligomerization-like receptors, glutathione S-transferase, propanoate metabolism, and so forth) are accounted for in the larger inflammation and metabolism pathways selected as most relevant. However, there were many genes related to other pathways, such as cytoplasm, acetylation, golgi apparatus, cofactor binding, and endoplasmic reticulum, which may also be relevant to the pathophysiology of sepsis but were not included in this analysis.

Integration Analysis of Lung Transcriptomics and Plasma Metabolomics

The transcriptomic data supported the hypothesis that mitochondrial dysfunction may lead to problems in β-oxidation and the increase in acyl-carnitines. We used a global cross-correlation analysis (8) between biologically linked metabolomes and transcriptomes to identify potential mechanistic associations. Because the metabolomic changes were dynamic in response to survival or death with the highest difference noted in nonsurvivors we decided to take an unbiased integrative analysis between high-dose survivors or nonsurvivors. The results focus on correlation of change rather than changes specific to outcome. We selected the 15 functional pathways identified by DAVID that relate to mitochondrial function, lipid oxidation, inflammation, and transcriptional regulation. These pathways encompass a total of 331 differentially expressed genes. All pairwise correlations, using Pearson product-moment correlation, are calculated for every gene with every significantly different metabolite (n = 233). Potentially relevant gene-by-metabolite associations were determined by r^2 values ($0.65 \geqslant$ or $\leqslant -0.65$) (*see* Table E4). Then for each gene, we calculated an average absolute value correlation for grouped biochemical families (e.g., TCA cycle metabolites) to determine genes that highly associate with metabolic pathways (*see* Table E5). DAVID pathway analysis is then used to cluster the relevant genes by function. Figure E1 presents a hypothetical integrative model of infection based on these gene-by-metabolite associations.

Known enzymatic reaction models should be identified by these gene-by-metabolite associations. Indeed, we found that kynureninase (*KYNU*) had high absolute value correlation (0.758) to the kynurenine pathway metabolites (*see* Table E6). We also noted that the kynurenine pathway metabolites strongly correlated to peroxisomal genes (*see* Figure E2). Interestingly, excreted terminally metabolized kynurenine metabolites are a marker for peroxisomal activation (32). Another finding identified by integrating the metabolomic and transcriptomic datasets is the strong correlation of TCA cycle intermediates succinate, malate, and fumarate to inflammatory response and cell death genes (Figure 5; *see* Figure E1, Tables E5 and E6). These data support a recent report that demonstrated LPS-challenged macrophages have increased succinate concentrations despite an overall decrease in TCA cycle respiration and that succinate leads to increased IL-1β production (33).

Acyl-GPCs and carnitine esters had a strong correlation to genes involved in BCAA-degradation, β-oxidation, and peroxisomal lipid oxidation (Figure 5; *see* Figure E1, and Tables E5 and E6). Decreased gene expression in these pathways likely leads to an accumulation of upstream metabolic intermediates; this may explain the observed rise in carnitine esters. We previously noted that acyl-GPC concentrations are lowered following infectious challenge (8). Interestingly, we found a strong negative correlation with lysophosphatidylcholine acyltransferase 2 (*LPCAT2*), which can recycle acyl-GPCs to phosphatidylcholine or acetylate acyl-GPCs to form platelet-activating factors after LPS stimulation (34). Many of the metabolite families strongly correlated with transcription factors known to regulate peroxisome activation, mitochondrial function, and fatty acid oxidation (*PPARG*, *PPARG* coactivator 1α [*PPARGC1A*] and *forkhead box O3* [*FOXO3*]) (Figure 5; *see* Figure E1, Tables E5 and E6). The decreased expression of PPARGC1A, which is a master coactivator of the peroxisomal proliferator-activated receptor (PPAR) pathway, along with the other PPAR-associated transcription factors may explain the decreased expression of peroxisomal and β-oxidation related genes that we and others have observed (35–40).

Identification of Sepsis Using Metabolomic Differences in Low- and High-Dose Challenges

The metabolome demonstrated dynamic temporal changes in response to infection. We therefore sought to build logistic regression models to diagnose infection. Time points constituting "noninfection" included baseline (n = 20) and convalescence (5-d low-dose, n = 12; 5-d high-dose, n = 3). Time points from animals that were symptomatic defined "infection" (1-d low-dose, n = 7; 3-d low-dose, n = 7; 3-d high-dose, n = 4; death, n = 4). We found that 1-stearoyl-GPC, kynurenine, and isovalerylcarnitine were highly accurate for determination of an infection (area under the curve [AUC], 0.9519, 0.9143, 0.8987, respectively) (Table 1). We then derived a four-metabolite logistic regression model using 1-stearoyl-GPC, kynurenine, isovalerylcarnitine, and taurolithocholate-3-sulfate to identify infection versus noninfection. These metabolites were selected based on the relationship to the pathophysiology of the disease and their high individual sensitivity. Although taurolithocholate-3-sulfate did not perform as well in diagnosis (AUC, 0.7695) it was included in the panel because of the reported relationship with liver cholestasis and patient outcome (30). The four-metabolite model performed similarly to 1-stearoyl-GPC alone (AUC, 0.9675 vs. 0.9519) (Table 1). Within the training set, incorrect model classifications were noted primarily

Figure 4. (Continued). challenge versus nonsurvivor, and high-dose challenge versus nonsurvivor; 82 genes were significantly different in control versus the other groups (high dose, low dose, or nonsurvivor) that were not significantly different in the other comparisons. (*C*) Heatmap of significant gene transcript abundance differences for control (CON; n = 2), sepsis low-dose challenge (n = 8), sepsis high-dose challenge (n = 4), and sepsis death (n = 4). (*D*) DAVID analysis. Official gene symbols for significant genes, minus duplicates and unknown Ensembl-reported genes, were uploaded into DAVID v6.7. The *Homo sapiens* gene list was used for functional annotation analysis. The analysis found 109 gene pathways significantly enriched ($P \leqslant 0.006$; false discovery rate $\leqslant 10$) (*see* Table E4). Fifteen metabolomic, inflammatory, and transcription factor enriched pathways are presented.

during convalescence. We next tested the four-metabolite training model on the RoCI and CAPSOD clinical cohorts, which had similar metabolomic measurements (8, 15). Noninfected SIRS and sepsis differentiation of the CAPSOD and RoCI cohorts has been described in detail (8, 11–13, 15). Sepsis included all patients regardless of final outcome (sepsis, severe sepsis, septic shock, and sepsis nonsurvivors). The four-metabolite NHP model tested well in two of three human metabolomic datasets (RoCI AUC, 0.7858; CAPSOD enrollment at hospital presentation AUC, 0.6672; CAPSOD 24-h postenrollment AUC, 0.8213). The results suggest these metabolites can differentiate SIRS from sepsis with reasonable confidence and there are conserved mechanisms in sepsis pathophysiology between NHP and humans.

Discussion

In this study, we used an integrative approach to identify diagnostic metabolites in sepsis pathogenesis in an experimental NHP model. Our results suggest mitochondrial dysfunction leads to severe infection and poor outcomes as demonstrated by changes to TCA cycle intermediates, decreased β-oxidation, and decreased lipid peroxisome activation. The metabolomic signatures were used to construct a four-metabolite panel that classifies sepsis diagnosis in two human clinical cohorts.

The infection model was based on the *E. coli* infection model developed by Welty-Wolf and coworkers (16). This model was selected over a single-infusion model because it leads to lung injury with less lethality (17, 18). We noted bacterial growth in plasma, lungs, spleen, and kidney in some low-dose and all high-dose challenges and dose-dependent lung injury and mortality. The metabolomic analysis demonstrated strong similarity to human sepsis, noting metabolomic increases in acyl-carnitines, kynurenine, bile acids, steroids, and TCA intermediates, and decreased acyl-GPCs. Many of these pathways have been highlighted in other sepsis studies (8, 27–30). Perhaps most impressive was the dynamic changes to these metabolites during peak infection, convalescence, and death in both low- and high-dose challenges.

To better elucidate what enzymatic or signaling pathways influenced the concentration of these metabolomic markers we performed a transcriptomic analysis of lung RNA. The lung was chosen because pulmonary disease often accompanies sepsis either in the form of primary pneumonia or secondary acute respiratory distress syndrome (2, 41). Furthermore, the experimental model

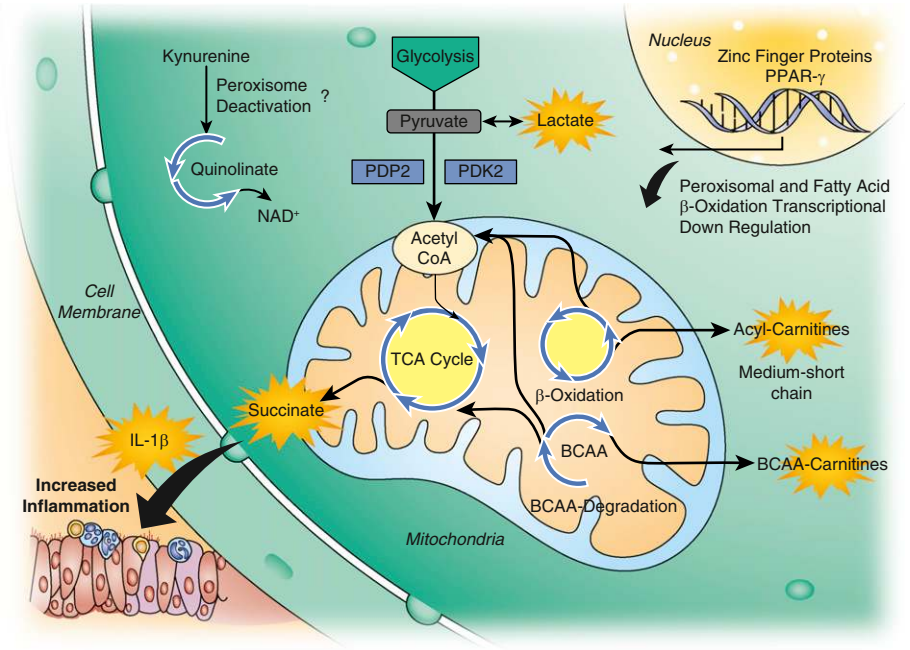

Figure 5. Hypothetical pathway analysis depicts mitochondrial dysfunction. Gene-by-metabolite associations highlight problems with tricarboxylic acid (TCA) cycle regulation, β-oxidation, branched-chain amino acid (BCAA) degradation, and peroxisomal activation likely leading to increased production of various acyl-carnitines, a strong predictive signature of poor sepsis outcomes. This mitochondrial dysregulation is likely mediated by peroxisomal proliferator-activated receptor-γ family transcription factors and/or novel zinc finger proteins. Problems with lipid metabolism are manifest in the strong association of kynurenine family metabolites and peroxisomal deactivation. Perhaps most interesting is the association of succinate with inflammatory gene *IL-1β*, suggesting a potential link to mitochondrial dysfunction and initiation of the inflammatory response. Nicotinamide adenine dinucleotide (NAD+); key TCA cycle rate-limiting enzymes pyruvate dehydrogenase phosphatase 2 (*PDP2*) and pyruvate dehydrogenase kinase 2 (*PDK2*) were down-regulated in high-dose challenges and nonsurvivors.

Table 1. Four-Metabolite Prediction Analysis

	AUC	RMSE	Accuracy (%)	PPV (%)	NPV (%)
Sepsis diagnosis					
Kynurenine	0.9143	0.3657	80.7	88.6	68.2
Isovalerylcarnitine	0.8987	0.3728	80.7	91.4	63.6
Taurolithocholate-3 sulfate	0.7695	0.3928	79.0	88.6	63.6
1-Stearoyl-GPC	0.9519	0.2887	89.5	91.4	86.4
Sepsis diagnosis*					
NHP (training)	0.9675	0.2699	89.5	91.4	86.4
RoCI (test)	0.7858	0.5397	67.8	96.6	54.1
CAPSOD t0 (test)	0.6672	0.6593	47.6	86.2	38.3
CAPSOD t24 (test)	0.8213	0.5929	58.3	100.0	48.6

Definition of abbreviations: AUC = area under the curve; CAPSOD = Community-acquired Pneumonia and Sepsis Outcomes Diagnostic; NHP = nonhuman primates; NPV = negative predictive value; PPV = positive predictive value; RMSE = root mean square error; RoCI = Registry of Critical Illness. Sepsis diagnosis, PPV = no infection (n = 35); NPV = infection (n = 22).
*Four-metabolite model (kynurenine, isovalerylcarnitine, taurolithocholate-3 sulfate, 1-stearoyl-glycerophosphocholine). RoCI: systemic inflammatory response syndrome (n = 29), sepsis (n = 61). CAPSOD t0: systemic inflammatory response syndrome (n = 29), sepsis (n = 120). CAPSOD t24: systemic inflammatory response syndrome (n = 25), sepsis (n = 107).

selected herein has a propensity to cause acute lung injury. We used RNAseq because of the dynamic range and high correlations to quantitative polymerase chain reaction (42). The analysis found 1,544 genes were significantly different. DAVID highlighted 15 pathways that were related to metabolomic regulation, mitochondrial function, inflammation, and transcriptional regulation.

To understand how these 331 genes from the 15 pathways may relate to the metabolome, we used global cross-correlation to integrate the two datasets. We hypothesized that both known and novel enzymatic reactions would strongly associate. We previously demonstrated that metabolites cluster together based on their metabolic similarity (e.g., acyl-carnitines cluster with other acyl-carnitines, steroids with other steroids, TCA cycle intermediates with other TCA cycle intermediates [8]). With this knowledge, we calculated the absolute value correlation of family metabolites to all 331 genes. This allowed for the discovery of known interactions, such as kynurenine with *KYNU*; suspected interactions, such as BCAA-carnitines with genes related to the valine, leucine, and isoleucine degradation pathway; and carnitine esters with β-oxidation genes. The novel findings presented herein suggest that mitochondrial dysfunction leads to an increase in carnitine esterification and that it seems to be a coordinated genomic signaling response in affected tissues.

Interestingly, the analysis also highlighted some unexpected interactions. We initially suspected changes in TCA intermediates would correlate with TCA-associated genes. Surprisingly, other than modification of the key rate-limiting enzymes, pyruvate dehydrogenase phosphate 2 (*PDP2*) and pyruvate dehydrogenase kinase 2 (*PDK2*), no significant TCA metabolite to TCA-associated gene correlations was found. However, there was strong correlation of the TCA intermediates to proinflammatory genes. It was recently demonstrated that succinate could initiate the production of IL-1β in bone marrow–derived macrophages by stabilization of HIF1α (33). Treating animals with vigabatrin, a γ-aminobutyric acid transaminase inhibitor that decreases succinate production, improved survival in LPS-challenged mice and reduced IL-1β in *Salmonella*-challenged mice. We found three PPAR-related transcription factors along with *THRA1* and the apoptosis-inducing gene *FOXO3* correlated with many of these significantly increased β-oxidation and peroxidation metabolites. Although untested here, we hypothesize PPAR agonists improve survival in septic mice (43–46) because of mitochondrial biogenesis leading to increased transcription of β-oxidation and BCAA-degradation associated genes. However, it should be noted that PPAR antiinflammatory effects have also been attributed to improved survival, and therefore links to mitochondrial function remains unclear. Future matched metabolomic, transcriptomic, and histopathologic analysis of individual tissue types (e.g., liver, kidney, heart muscle) would provide a more focused understanding of sepsis-induced changes at the organ level.

The highly dynamic changes in the metabolome during infection and convalescence in our experimental model suggested these markers could be used for clinical sepsis diagnosis. We selected four markers based on their changes over time and biologic plausibility (kynurenine and peroxidation; taurolithocholate-3-sulfate and liver dysfunction; acyl-carnitines and mitochondrial dysfunction; and acyl-GPC depletion as a potential marker for platelet activation). The model performed exceptionally well in the training set with incorrect prediction primarily noted during intermediate time points of convalescence. We validated this model in two human sepsis datasets, specifically the CAPSOD and RoCI cohorts. Differentiation of sepsis versus SIRS has been previously described (8, 11–13). We found that the model was good at discriminating infected from noninfected patients enrolled in the ICU (RoCI) and 24-hour post emergency department enrollment (CAPSOD t24). The model did not perform particularly well in emergency department enrollment (CAPSOD t0). This may reflect a heterogenic SIRS response that is nonspecific to infection. Earlier measurement of metabolomic changes in the NHP model and a measurement in a noninfected SIRS model may better inform the use of these diagnostic markers to diagnose sepsis. Previous studies have identified procalcitonin, IL-6, and C-reactive protein as putative markers of clinical sepsis. The current studies were not designed to compare these markers with those identified here. It should be noted that the novel markers identified here outperformed procalcitonin, IL-6, and C-reactive protein in the CAPSOD data as previously published by these investigators (12). The incorporation of procalcitonin, IL-6, and C-reactive protein may improve the prediction of sepsis by the novel markers reported here, and future investigations will seek to further refine the predictive model.

This study does have limitations. First, it is unclear how infection classification in NHPs relates to illness in humans: is it indicative of a mild or severe course? Second, it has been well documented that experimental models and clinical results are often incongruous. This is caused in part by differential genomic responses and clinical relevance of the experimental models (47, 48), and a heterogeneous response in humans related to site-of-infection, etiologic agent, genetics, comorbidities, and age-related confounders (2). However, the metabolomic changes found in the primate model strongly correlate to metabolomic findings noted in human sepsis. This suggests shared pathophysiology in the metabolomic response to severe infections. Future NHP studies that include clinical management similar to what patients would receive (e.g., antibiotic therapy and fluid resuscitation) would improve external validity. Third, we did not find any significant changes in lactate other than in the nonsurvivors. It is possible that lactate did not change in the survivors because they did not become hypotensive and were able to maintain adequate organ perfusion. This does suggest that despite many similarities to human sepsis, the sepsis model presented here has key differences likely caused by its highly controlled nature and limited duration of infection.

Finally, because we lacked noninfectious SIRS controls, it is unclear if the markers are unique for sepsis. Although the model was good at differentiating sepsis versus noninfectious SIRS in the human RoCI and CAPSOD cohorts, it is still possible some or all of the metabolites in our model are also perturbed in other forms of SIRS, such as trauma. Better clinical understanding of the metabolomic response in trauma and the development of a noninfected SIRS animal model will help to clarify this concern. Furthermore, future studies with denser sampling may provide information about early septic changes when diagnosis and interventions will have the greatest impact. As with any association study,

we cannot determine causality. However, known biologic pathways and published literature do inform likely mechanisms of interaction. Future mechanistic studies in other model systems are necessary. The strength of this study is that transcriptomic and metabolomic integration identified both known and novel mechanistic associations that may be targets for interventions.

These results highlight the strong association of metabolomic changes caused by an infectious challenge that can lead to death. The changes correlated with the human sepsis metabolome suggest the NHP sepsis model is useful for preclinical intervention studies. Therapeutic interventions targeting mitochondrial activation or biogenesis may improve outcomes in severe sepsis and septic shock. ■

Author disclosures are available with the text of this article at www.atsjournals.org.

Acknowledgment: The authors thank Tom Gagliano for graphic arts and the study subjects.

References

1. Angus DC, Linde-Zwirble WT, Lidicker J, Clermont G, Carcillo J, Pinsky MR. Epidemiology of severe sepsis in the United States: analysis of incidence, outcome, and associated costs of care. *Crit Care Med* 2001;29:1303–1310.
2. Angus DC, van der Poll T. Severe sepsis and septic shock. *N Engl J Med* 2013;369:840–851.
3. Liu V, Escobar GJ, Greene JD, Soule J, Whippy A, Angus DC, Iwashyna TJ. Hospital deaths in patients with sepsis from 2 independent cohorts. *JAMA* 2014;312:90–92.
4. Rivers E, Nguyen B, Havstad S, Ressler J, Muzzin A, Knoblich B, Peterson E, Tomlanovich M; Early Goal-Directed Therapy Collaborative Group. Early goal-directed therapy in the treatment of severe sepsis and septic shock. *N Engl J Med* 2001;345: 1368–1377.
5. Pea F, Viale P. Bench-to-bedside review: Appropriate antibiotic therapy in severe sepsis and septic shock—does the dose matter? *Crit Care* 2009;13:214.
6. Hranjec T, Sawyer RG. Conservative initiation of antimicrobial treatment in ICU patients with suspected ICU-acquired infection: more haste less speed. *Curr Opin Crit Care* 2013;19:461–464.
7. Hranjec T, Rosenberger LH, Swenson B, Metzger R, Flohr TR, Politano AD, Riccio LM, Popovsky KA, Sawyer RG. Aggressive versus conservative initiation of antimicrobial treatment in critically ill surgical patients with suspected intensive-care-unit-acquired infection: a quasi-experimental, before and after observational cohort study. *Lancet Infect Dis* 2012;12:774–780.
8. Langley RJ, Tsalik EL, Velkinburgh JC, Glickman SW, Rice BJ, Wang C, Chen B, Carin L, Suarez A, Mohney RP, *et al*. An integrated clinico-metabolomic model improves prediction of death in sepsis. *Sci Transl Med* 2013;5:195ra195.
9. Sauer U, Heinemann M, Zamboni N. Genetics. Getting closer to the whole picture. *Science* 2007;316:550–551.
10. Langley RJ, Tipper JL, Jaramillo RJ, O'Donnell D, Keaton M, Kensicki E, Baron RM, Perrella MA, Choi AMK, Harrod KS. Integrative 'omics analysis in a non-human primate model of sepsis highlights mitochondrial derangements in death [abstract]. *Am J Respir Crit Care Med* 2013;187:A1009.
11. Glickman SW, Cairns CB, Otero RM, Woods CW, Tsalik EL, Langley RJ, van Velkinburgh JC, Park LP, Glickman LT, Fowler VG Jr, *et al*. Disease progression in hemodynamically stable patients presenting to the emergency department with sepsis. *Acad Emerg Med* 2010; 17:383–390.
12. Tsalik EL, Jaggers LB, Glickman SW, Langley RJ, van Velkinburgh JC, Park LP, Fowler VG, Cairns CB, Kingsmore SF, Woods CW. Discriminative value of inflammatory biomarkers for suspected sepsis. *J Emerg Med* 2012;43:97–106.
13. Tsalik EL, Jones D, Nicholson B, Waring L, Liesenfeld O, Park LP, Glickman SW, Caram LB, Langley RJ, van Velkinburgh JC, *et al*. Multiplex PCR to diagnose bloodstream infections in patients admitted from the emergency department with sepsis. *J Clin Microbiol* 2010;48:26–33.
14. Dolinay T, Kim YS, Howrylak J, Hunninghake GM, An CH, Fredenburgh L, Massaro AF, Rogers A, Gazourian L, Nakahira K, *et al*. Inflammasome-regulated cytokines are critical mediators of acute lung injury. *Am J Respir Crit Care Med* 2012;185:1225–1234.
15. Rogers AJ, McGeachie M, Baron RM, Gazourian L, Haspel JA, Nakahira K, Fredenburgh LE, Hunninghake GM, Raby BA, Matthay MA, *et al*. Metabolomic derangements are associated with mortality in critically ill adult patients. *PLoS ONE* 2014;9:e87538.
16. Welty-Wolf KE, Carraway MS, Ortel TL, Ghio AJ, Idell S, Egan J, Zhu X, Jiao JA, Wong HC, Piantadosi CA. Blockade of tissue factor-factor X binding attenuates sepsis-induced respiratory and renal failure. *Am J Physiol Lung Cell Mol Physiol* 2006;290:L21–L31.
17. Welty-Wolf KE, Carraway MS, Huang YC, Simonson SG, Kantrow SP, Piantadosi CA. Bacterial priming increases lung injury in gram-negative sepsis. *Am J Respir Crit Care Med* 1998;158:610–619.
18. Welty-Wolf KE, Carraway MS, Miller DL, Ortel TL, Ezban M, Ghio AJ, Idell S, Piantadosi CA. Coagulation blockade prevents sepsis-induced respiratory and renal failure in baboons. *Am J Respir Crit Care Med* 2001;164:1988–1996.
19. Johnson TJ, Kariyawasam S, Wannemuehler Y, Mangiamele P, Johnson SJ, Doetkott C, Skyberg JA, Lynne AM, Johnson JR, Nolan LK. The genome sequence of avian pathogenic *Escherichia coli* strain O1:K1:H7 shares strong similarities with human extraintestinal pathogenic *E. coli* genomes. *J Bacteriol* 2007;189: 3228–3236.
20. Mora A, López C, Dabhi G, Blanco M, Blanco JE, Alonso MP, Herrera A, Mamani R, Bonacorsi S, Moulin-Schouleur M, *et al*. Extraintestinal pathogenic *Escherichia coli* O1:K1:H7/NM from human and avian origin: detection of clonal groups B2 ST95 and D ST59 with different host distribution. *BMC Microbiol* 2009;9:132.
21. Deitch EA. Animal models of sepsis and shock: a review and lessons learned. *Shock* 1998;9:1–11.
22. Huang W, Sherman BT, Lempicki RA. Systematic and integrative analysis of large gene lists using DAVID bioinformatics resources. *Nat Protoc* 2009;4:44–57.
23. Huang W, Sherman BT, Lempicki RA. Bioinformatics enrichment tools: paths toward the comprehensive functional analysis of large gene lists. *Nucleic Acids Res* 2009;37:1–13.
24. Storey JD. A direct approach to false discovery rates. *J R Stat Soc Series B Stat Methodol* 2002;64:479–498.
25. Storey JD, Taylor JE, Siegmund D. Strong control, conservative point estimation and simultaneous conservative consistency of false discovery rates: a unified approach. *J R Stat Soc Series B Stat Methodol* 2004;66:187–205.
26. Dellinger RP, Levy MM, Carlet JM, Bion J, Parker MM, Jaeschke R, Reinhart K, Angus DC, Brun-Buisson C, Beale R, *et al*.; International Surviving Sepsis Campaign Guidelines Committee; American Association of Critical-Care Nurses; American College of Chest Physicians; American College of Emergency Physicians; Canadian Critical Care Society; European Society of Clinical Microbiology and Infectious Diseases; European Society of Intensive Care Medicine; European Respiratory Society; International Sepsis Forum; Japanese Association for Acute Medicine; Japanese Society of Intensive Care Medicine; Society of Critical Care Medicine; Society of Hospital Medicine; Surgical Infection Society; World Federation of Societies of Intensive and Critical Care Medicine. Surviving Sepsis Campaign: international guidelines for management of severe sepsis and septic shock: 2008. *Crit Care Med* 2008;36:296–327.
27. Drobnik W, Liebisch G, Audebert FX, Frohlich D, Gluck T, Vogel P, Rothe G, Schmitz G. Plasma ceramide and lysophosphatidylcholine inversely correlate with mortality in sepsis patients. *J Lipid Res* 2003; 44:754–761.

28. Yan JJ, Jung JS, Lee JE, Lee J, Huh SO, Kim HS, Jung KC, Cho JY, Nam JS, Suh HW, *et al*. Therapeutic effects of lysophosphatidylcholine in experimental sepsis. *Nat Med* 2004;10:161–167.
29. Weiner J III, Parida SK, Maertzdorf J, Black GF, Repsilber D, Telaar A, Mohney RP, Arndt-Sullivan C, Ganoza CA, Faé KC, *et al*. Biomarkers of inflammation, immunosuppression and stress with active disease are revealed by metabolomic profiling of tuberculosis patients. *PLoS ONE* 2012;7:e40221.
30. Recknagel P, Gonnert FA, Westermann M, Lambeck S, Lupp A, Rudiger A, Dyson A, Carré JE, Kortgen A, Krafft C, *et al*. Liver dysfunction and phosphatidylinositol-3-kinase signalling in early sepsis: experimental studies in rodent models of peritonitis. *PLoS Med* 2012;9:e1001338.
31. Zhang W, Huang RS, Duan S, Dolan ME. Gene set enrichment analyses revealed differences in gene expression patterns between males and females. *In Silico Biol* 2009;9:55–63.
32. Ringeissen S, Connor SC, Brown HR, Sweatman BC, Hodson MP, Kenny SP, Haworth RI, McGill P, Price MA, Aylott MC, *et al*. Potential urinary and plasma biomarkers of peroxisome proliferation in the rat: identification of N-methylnicotinamide and N-methyl-4-pyridone-3-carboxamide by 1H nuclear magnetic resonance and high performance liquid chromatography. *Biomarkers* 2003;8:240–271.
33. Tannahill GM, Curtis AM, Adamik J, Palsson-McDermott EM, McGettrick AF, Goel G, Frezza C, Bernard NJ, Kelly B, Foley NH, *et al*. Succinate is an inflammatory signal that induces IL-1β through HIF-1α. *Nature* 2013;496:238–242.
34. Morimoto R, Shindou H, Oda Y, Shimizu T. Phosphorylation of lysophosphatidylcholine acyltransferase 2 at Ser34 enhances platelet-activating factor production in endotoxin-stimulated macrophages. *J Biol Chem* 2010;285:29857–29862.
35. Mandard S, Müller M, Kersten S. Peroxisome proliferator-activated receptor alpha target genes. *Cell Mol Life Sci* 2004;61:393–416.
36. Feingold K, Kim MS, Shigenaga J, Moser A, Grunfeld C. Altered expression of nuclear hormone receptors and coactivators in mouse heart during the acute-phase response. *Am J Physiol Endocrinol Metab* 2004;286:E201–E207.
37. Feingold KR, Moser A, Patzek SM, Shigenaga JK, Grunfeld C. Infection decreases fatty acid oxidation and nuclear hormone receptors in the diaphragm. *J Lipid Res* 2009;50:2055–2063.
38. Kim MS, Shigenaga JK, Moser AH, Feingold KR, Grunfeld C. Suppression of estrogen-related receptor alpha and medium-chain acyl-coenzyme A dehydrogenase in the acute-phase response. *J Lipid Res* 2005;46:2282–2288.
39. Djouadi F, Bastin J. PPARalpha gene expression in the developing rat kidney: role of glucocorticoids. *J Am Soc Nephrol* 2001;12: 1197–1203.
40. Feingold KR, Wang Y, Moser A, Shigenaga JK, Grunfeld C. LPS decreases fatty acid oxidation and nuclear hormone receptors in the kidney. *J Lipid Res* 2008;49:2179–2187.
41. Del Sorbo L, Slutsky AS. Acute respiratory distress syndrome and multiple organ failure. *Curr Opin Crit Care* 2011;17:1–6.
42. Wang Z, Gerstein M, Snyder M. RNA-Seq: a revolutionary tool for transcriptomics. *Nat Rev Genet* 2009;10:57–63.
43. Wiel E, Lebuffe G, Robin E, Gasan G, Corseaux D, Tavernier B, Jude B, Bordet R, Vallet B. Pretreatment with peroxysome proliferator-activated receptor alpha agonist fenofibrate protects endothelium in rabbit *Escherichia coli* endotoxin-induced shock. *Intensive Care Med* 2005;31:1269–1279.
44. Kapoor A, Shintani Y, Collino M, Osuchowski MF, Busch D, Patel NS, Sepodes B, Castiglia S, Fantozzi R, Bishop-Bailey D, *et al*. Protective role of peroxisome proliferator-activated receptor-β/δ in septic shock. *Am J Respir Crit Care Med* 2010;182: 1506–1515.
45. Zingarelli B, Piraino G, Hake PW, O'Connor M, Denenberg A, Fan H, Cook JA. Peroxisome proliferator-activated receptor delta regulates inflammation via NF-kappaB signaling in polymicrobial sepsis. *Am J Pathol* 2010;177:1834–1847.
46. Wu WT, Lee CC, Lee CJ, Subeq YM, Lee RP, Hsu BG. Rosiglitazone ameliorates endotoxin-induced organ damage in conscious rats. *Biol Res Nurs* 2011;13:38–43.
47. Seok J, Warren HS, Cuenca AG, Mindrinos MN, Baker HV, Xu W, Richards DR, McDonald-Smith GP, Gao H, Hennessy L, *et al*.; Inflammation and Host Response to Injury, Large Scale Collaborative Research Program. Genomic responses in mouse models poorly mimic human inflammatory diseases. *Proc Natl Acad Sci USA* 2013; 110:3507–3512.
48. Fink MP. Animal models of sepsis. *Virulence* 2014;5:143–153.